Non-rigid Object Segmentation Using Robust Active Shape Models

Carlos Santiago*, Jacinto C. Nascimento, and Jorge S. Marques

ISR, Instituto Superior Técnico
Lisbon, Portugal
carlos.santiago@ist.utl.pt

Abstract. Statistical shape models have been extensively used in several image analysis problems, providing accurate estimates of object boundaries. However, their performance degrades if the object of interest is surrounded by a cluttered background, and the features extracted from the image contain outliers. Under these assumptions, most deformable models fail since they are attracted towards the outliers, leading to poor shape estimates. This paper proposes a *robust Active Shape Model*, based on a sensor model that takes into account both valid and invalid observations. A weight (*confidence degree*) is assigned to each observation. All the observations contribute to the estimation of the object boundary but with different weights. The estimation process is recursively performed by the Expectation-Maximization method and the weights are updated in each iteration. The algorithm was tested in ultrasound images of the left ventricle and compared with the output of classic Active Shape Models. The proposed algorithm performs significantly better.

1 Introduction

The segmentation of human organs in medical images is a challenging problem that has been addressed in several ways. Deformable models are amongst the most popular approaches since they separate geometric modeling of the contour from the visual features of the organ and background. Active Shape Models (ASMs) proposed in [1] are especially interesting since the shape model is trained from annotated data and the model learns not only the average shape of the object but also its deformation modes. This information is conveyed in a Gaussian prior that improves contour estimates and avoids unusual shapes.

Active Shape Models have been improved with respect to the way information is extracted from the image, trying to obtain more reliable features [2–7]. However, if the model is initialized far from the object contour and if the background is textured, a high number of outliers may be observed, attracting the elastic contour towards erroneous configurations. The performance of ASMs is therefore

* This work was supported in part by the FCT project [PEst-OE/EEI/LA0009/2013], by project "HEARTRACK"- PTDC/EEA-CRO/103462/2008 and under the FCT scholarship SFRH/BD/87347/2012.

F.J. Perales and J. Santos-Victor (Eds.): AMDO 2014, LNCS 8563, pp. 160–169, 2014.
© Springer International Publishing Switzerland 2014

hampered by invalid features since the model is not robust in the presence of outliers

Few works tried to address the robustness of ASMs. One notable exception is the work of Rogers et al. [8], which tries to overcome this problem by using a random sampling consensus method, RANSAC [9]. Another contribution to improve robustness was proposed by Nahed et al. [10] based on Robust Point Matching (RPM)[11] which tries to solve the matching problem between model points and observation points detected in the image. This algorithm is able to discard the observations considered as outliers in the matching process.

In this paper, we propose an alternative approach to estimate the ASM parameters in cluttered images. We explicitly assume that the feature points detected in the image contain outliers which do not belong to the object boundary. Each observation is associated to a binary label (valid/invalid) which is unknown; different sensor models are adopted to describe valid data and outliers. The estimation of the model parameters (global motion and shape deformation) in the presence of unobserved variables (binary labels) is carried out by the Expectation-Maximization method. The method developed in this paper is inspired in the work presented in [12] to improve the robustness of the snake algorithm. Experiments with ultrasound sequences of the heart show that the proposed method performs better that classic ASM in these experiments.

The remainder of this paper is organized as follows: Section 2 describes the problem and the proposed model; Section 3 describes parameter estimation by the Expectation-Maximization method; the application to ultrasound images of the heart is described in Section 4; and Section 5 concludes the paper.

2 Problem Formulation

Active Shape Models (ASM) [1] try to approximate the boundary of objects in images by sequences of 2D points (landmarks), $\mathbf{x} = (\mathbf{x}^1, \ldots, \mathbf{x}^N)$ with $\mathbf{x}^i \in \mathbb{R}^2$. Since the model is very flexible, a probabilistic model is adopted to constrain the set of admissible shapes. The 2D points are considered as a realization of random variables with joint Gaussian distribution, characterized by an average shape, $\bar{\mathbf{x}}$, and by a covariance matrix, $\mathbf{R}$. The covariance matrix defines the deformation modes that can be obtained by principal component analysis (PCA) $\mathbf{R} = \mathbf{W}\boldsymbol{\Lambda}\mathbf{W}^T$ where $\mathbf{W}$ is a matrix of eigenvectors and $\boldsymbol{\Lambda}$ is a diagonal matrix of eigenvalues, λ_k. The average shape and the deformation modes are estimated in a two-stage training process involving [1]: (i) alignment of all training shapes and (ii) Principal Component Analysis (PCA).

This leads to a generative shape model in which the object contour is randomly generated by

$$\mathbf{x} \simeq \bar{\mathbf{x}} + \mathbf{D}\mathbf{b} \ , \tag{1}$$

where $\mathbf{D} \in \mathbb{R}^{2N \times K}$ is a matrix with K main deformation modes extracted from $\mathbf{W}$, and $\mathbf{b} \in \mathbb{R}^K$ is a Gaussian vector of coefficients (local deformation).

In addition, the contour undergoes a geometric transformation $\mathbf{T}_{\boldsymbol{\theta}}$ (Euclidean similarity): each contour point is transformed by

$$\widetilde{\mathbf{x}}^i = \mathbf{T}_{\boldsymbol{\theta}}(\mathbf{x}^i) = \mathbf{A}(\bar{\mathbf{x}}^i + \mathbf{D}^i\mathbf{b}) + \mathbf{t} \ , \tag{2}$$

where $\mathbf{D}^i \in \mathbb{R}^{2\times K}$ is the mode deformation matrix associated to the $i-th$ landmark and $\boldsymbol{\theta} = (\mathbf{A}, \mathbf{t})$ are the transformation parameters (global motion).

When we wish to estimate the boundary of an object in a test image, an initial contour, $\widetilde{\mathbf{x}} = (\widetilde{\mathbf{x}}^1, \ldots, \widetilde{\mathbf{x}}^N)$, is required to initiate the estimation process. Then, we search for edges (intensity transitions) along search lines orthogonal to the contour at each model point $\widetilde{\mathbf{x}}^i$. Edge detection is performed along each line providing a set of edge points $\mathbf{Y}^i = \{\mathbf{y}^{ij}, j = 1, \ldots, M^i\}$. Multiple edges are detected in each line and many of them are outliers. Therefore, a binary label $k^{ij} \in \{0, 1\}$ is assigned to each edge point. We define $k^{ij} = 1$, if $\mathbf{y}^{ij}$ is a valid observation and $k^{ij} = 0$, otherwise. The probabilities of invalid and valid data $p_0 = P(k^{ij} = 0), p_1 = P(k^{ij} = 1)$ need to be estimated. Therefore, the model parameters comprise: global transformation parameters, local deformation parameters and the sensor probabilities $\boldsymbol{\psi} = (\boldsymbol{\theta}, \mathbf{b}, \mathbf{p})$, with $\mathbf{p} = (p_0, p_1)$.

Two sensor models will be considered. If an observation $\mathbf{y}^{ij}$ is valid ($k^{ij} = 1$), we assume that

$$\mathbf{y}^{ij} = \widetilde{\mathbf{x}}^i + \mathbf{v}^i = \mathbf{A}(\bar{\mathbf{x}}^i + \mathbf{D}^i\mathbf{b}) + \mathbf{t} + \mathbf{v}^i \tag{3}$$

where $\mathbf{v}^i \sim \mathcal{N}(\mathbf{0}, {\sigma^i}^2\mathbf{I})$ is a Gaussian random variable with zero mean and variance $(\sigma^i)^2\mathbf{I}$, estimated from the training set. Therefore,

$$p\left(\mathbf{y}^{ij}\middle|k^{ij}{=}1\right) = \mathcal{N}\left(\mathbf{y}^{ij}; \mathbf{A}(\bar{\mathbf{x}}^i + \mathbf{D}^i\mathbf{b}) + \mathbf{t}, (\sigma^i)^2\mathbf{I}\right). \tag{4}$$

If the observation $\mathbf{y}^{ij}$ is invalid ($k^{ij} = 0$), we assume it follows a uniform distribution $\mathcal{U}(V_{\widetilde{\mathbf{x}}^i})$ within a validation gate $V_{\widetilde{\mathbf{x}}^i}$ in the vicinity of $\widetilde{\mathbf{x}}^i$, i.e. $p\left(\mathbf{y}^{ij}\middle|k^{ij}{=}0\right) = \mathcal{U}(V_{\mathbf{x}^i})$.

These sensor models allow us to write a generative model for the observed data. Let $\mathbf{Y} = \{\mathbf{y}^{ij}\}$ be the set of all observations and $\mathbf{K} = \{k^{ij}\}$ the hidden labels. Assuming conditional independence, the complete likelihood function is given by

$$p(\mathbf{Y}, \mathbf{K}|\boldsymbol{\psi}) = \prod_{i=1}^{N}\prod_{j=1}^{M^i} p(\mathbf{y}^{ij}|k^{ij}\boldsymbol{\psi})p(k^{ij}) \ . \tag{5}$$

The likelihood function $p(\mathbf{Y}|\boldsymbol{\psi})$ is obtained by marginalizing $p(\mathbf{Y}, \mathbf{K}|\boldsymbol{\psi})$ with respect to the hidden variables $\mathbf{K}$, leading to

$$p(\mathbf{Y}|\boldsymbol{\psi}) = \sum_{\mathbf{K}} p(\mathbf{Y}, \mathbf{K}|\boldsymbol{\psi}) \ . \tag{6}$$

This marginalization step is unfeasible in practice since the number of configurations of the variables $\mathbf{K}$ grows exponentially with the number of unknown labels. A direct estimation of the model parameters $\boldsymbol{\psi}$ by the Maximum Likelihood Method is unfeasible. Fortunately, this difficulty can be solved by using the Expectation-Maximization method.

3 Expectation Maximization Framework

Instead of maximizing the likelihood function (6), we use the Expectation-Maximization (EM) method [13]. The EM method computes an auxiliary function $Q(.,.)$ (E-step) and updates the parameter estimates $\widehat{\boldsymbol{\psi}}$ by maximizing the auxiliary function (M-step). These two steps are repeated until convergence is achieved.

3.1 E-step

The auxiliary function $Q(.,.)$ is defined as the expected value of the complete log-likelihood function, given the observations $\mathbf{Y}$ and the most recent estimates of the parameters $\widehat{\boldsymbol{\psi}}$

$$Q\left(\boldsymbol{\psi}, \widehat{\boldsymbol{\psi}}\right) = \mathbb{E}_{\mathbf{K}}\left[\log p\left(\mathbf{Y}, \mathbf{K}|\boldsymbol{\psi}\right)\Big|\mathbf{Y}, \widehat{\boldsymbol{\psi}}\right] \quad . \tag{7}$$

The log-likelihood function is given by (see (5))

$$\log p\left(\mathbf{Y}, \mathbf{K}|\boldsymbol{\psi}\right) = \sum_{i=1}^{N}\sum_{j=1}^{M_i} \log p\left(\mathbf{y}^{ij}\big|k^{ij}, \boldsymbol{\psi}\right) + \log p\left(k^{ij}\right).$$

Therefore,

$$\begin{aligned} Q\left(\boldsymbol{\psi}, \widehat{\boldsymbol{\psi}}\right) = \sum_{i=1}^{N}\sum_{j=1}^{M_i} & w_0^{ij}\left[\log p\left(\mathbf{y}^{ij}\big|k^{ij}{=}0, \boldsymbol{\psi}\right) + \log p_0\right] \\ & + w_1^{ij}\left[\log p\left(\mathbf{y}^{ij}\big|k^{ij}{=}1, \boldsymbol{\psi}\right) + \log p_1\right], \end{aligned} \tag{8}$$

with

$$w_1^{ij} = p\left(k^{ij}{=}1\Big|\mathbf{y}^{ij}, \widehat{\boldsymbol{\psi}}\right) \propto \widehat{p}_1\, \mathcal{N}\left(\mathbf{y}^{ij}; \mathbf{T}_{\widehat{\boldsymbol{\theta}}}(\bar{\mathbf{x}}^i + \mathbf{D}^i\widehat{\mathbf{b}}), {\sigma^i}^2\mathbf{I}\right) \tag{9}$$

and $w_0^{ij} = p\left(k^{ij}{=}0\big|\mathbf{y}^{ij}\right) = \widehat{p}_0\, \mathcal{U}\left(V_{\mathbf{x}^i}\right)$ such that $w_0^{ij} + w_1^{ij} = 1$. These weights correspond to the probability of the observation being a valid observation or an outlier.

3.2 M-step

Let us assume that the most recent estimates of the unknown parameters in iteration $t-1$ are given by $\widehat{\boldsymbol{\psi}}(t-1)$. Parameter update is achieved by solving the following optimization problem

$$\widehat{\boldsymbol{\psi}}(t) = \arg\max_{\boldsymbol{\psi}}\ Q(\boldsymbol{\psi}, \widehat{\boldsymbol{\psi}}(t-1)) \tag{10}$$

The maximization with respect to $\boldsymbol{\psi} = (\boldsymbol{\theta}, \mathbf{b}, \mathbf{p})$ is performed in three steps that will be described in the sequel.

Estimation of $\boldsymbol{\theta}$: First we optimize the auxiliary function $Q(.,.)$ with respect to $\mathbf{A} = \begin{bmatrix} a_1 & -a_2 \\ a_2 & a_1 \end{bmatrix}, \mathbf{t} = \begin{bmatrix} t_1 \\ t_2 \end{bmatrix}$. The optimization can be analytically done and leads to a linear system of equations

$$\begin{pmatrix} X_1 & -X_2 & W & 0 \\ X_2 & X_1 & 0 & W \\ Z & 0 & X_1 & X_2 \\ 0 & Z & -X_2 & X_1 \end{pmatrix} \begin{pmatrix} \widehat{a}_1(t) \\ \widehat{a}_2(t) \\ \widehat{t}_1(t) \\ \widehat{t}_2(t) \end{pmatrix} = \begin{pmatrix} Y_1 \\ Y_2 \\ C_1 \\ C_2 \end{pmatrix}, \tag{11}$$

where

$$\begin{aligned} X_1 &= \sum_{i=1}^{N} \sum_{j=1}^{M_i} \frac{w_1^{ij}}{{\sigma^i}^2} x_1^i & Z &= \sum_{i=1}^{N} \sum_{j=1}^{M_i} \frac{w_1^{ij}}{{\sigma^i}^2} ({x_1^i}^2 + {x_2^i}^2) \\ X_2 &= \sum_{i=1}^{N} \sum_{j=1}^{M_i} \frac{w_1^{ij}}{{\sigma^i}^2} x_2^i & W &= \sum_{i=1}^{N} \sum_{j=1}^{M_i} \frac{w_1^{ij}}{{\sigma^i}^2} \\ Y_1 &= \sum_{i=1}^{N} \sum_{j=1}^{M_i} \frac{w_1^{ij}}{{\sigma^i}^2} y_1^{ij} & C_1 &= \sum_{i=1}^{N} \sum_{j=1}^{M_i} \frac{w_1^{ij}}{{\sigma^i}^2} (x_1^i y_1^{ij} + x_2^i y_2^{ij}) \\ Y_2 &= \sum_{i=1}^{N} \sum_{j=1}^{M_i} \frac{w_1^{ij}}{{\sigma^i}^2} y_2^{ij} & C_2 &= \sum_{i=1}^{N} \sum_{j=1}^{M_i} \frac{w_1^{ij}}{{\sigma^i}^2} (x_1^i y_2^{ij} - x_2^i y_1^{ij}) \ . \end{aligned}$$

Estimation of b: To update the deformation parameters, we maximize $Q(.,.)$ with respect to $\mathbf{b}$. This leads again to a linear system of equations

$$\left(\sum_{i=1}^{N} \sum_{j=1}^{M_i} \frac{w_1^{ij}}{{\sigma^i}^2} {\mathbf{D}^i}^\top \widehat{\mathbf{A}}^\top \widehat{\mathbf{A}} \mathbf{D}^i \right) \widehat{\mathbf{b}}(t) = \left(\sum_{i=1}^{N} \sum_{j=1}^{M_i} \frac{w_1^{ij}}{{\sigma^i}^2} {\mathbf{D}^i}^\intercal \widehat{\mathbf{A}}^\top \left[\mathbf{y}^{ij} - \widehat{\mathbf{A}} \bar{\mathbf{x}}^i - \widehat{\mathbf{t}} \right] \right) . \tag{12}$$

The deformation parameters obtained from (12) may correspond to an unexpected shape. Therefore, we use the protection mechanism proposed in [1]. First we compute the Mahalanobis distance, d, and compare it to threshold, $d_{\max}$,

$$d^2 = \sum_{l=1}^{K} \frac{\widehat{b}_l^2}{\lambda_l} \leq d_{\max}^2. \tag{13}$$

where $\widehat{b}_l$ denotes the l-th component of $\widehat{\mathbf{b}}$, and λ_l is the eigenvalue associated to the l-th deformation mode. The threshold is chosen so that most of the shapes in the training set satisfy (13) (a typical value is $d_{\max} = 3$ [1]). If $\widehat{\mathbf{b}}$ does not satisfy (13), we rescale it as follows

$$\widehat{\mathbf{b}}(t) \leftarrow \widehat{\mathbf{b}}(t)\frac{d_{\max}}{d} \quad , \qquad \text{if } d > d_{\max}. \tag{14}$$

Estimation of p: Finally, we update the probabilities of valid and invalid data by maximizing $Q(.,.)$ with respect to p_0, p_1. This yields

$$\widehat{p}_1(t) = \frac{\sum_{i=1}^{N}\sum_{j=1}^{M_i} w_1^{ij}}{\sum_{i=1}^{N}\sum_{j=1}^{M_i} w_1^{ij} + w_0^{ij}} \quad , \qquad \widehat{p}_0(t) = 1 - \widehat{p}_1(t) \ . \tag{15}$$

The shape estimation algorithm described in this section will be denoted as **EM Robust Active Shape Model (EM-RASM)**.

4 Experimental Evaluation

This section shows examples and statistical results of the EM-RASM method applied to the segmentation of the endocardium of the left ventricle in ultrasound images.

In all the tests, the model was initialized with the average shape $\bar{\mathbf{x}}$ (i.e., $\mathbf{b} = \mathbf{0}$). The initial guess for the transformation parameters was obtained by aligning the average shape $\bar{\mathbf{x}}$ with a contour obtained by human input using the standard least squares method. The initial guess for the models probabilities was $p_0 = p_1 = 0.5$. We found no evidence suggesting that the initial values for these probabilities significantly changed the output of the algorithm.

In this work, the observation points were obtained by searching for edge points along lines orthogonal to the contour at each model point. The feature detection algorithm used was a matched filter designed for edge detection (see [14], Section 5.2). This detector convolves the intensity profile along each search line with an edge operator. Edge points correspond to the maxima of the filtered signal that can be detected by applying thresholding followed by non-maximum suppression. The threshold allows us to modify the sensitivity of the edge detector, which may depend on the application. The length of the search line is also application-dependent since it depends on the uncertainty associated to the contour.

The standard ASM [1] performs a similar search method, but the observation points correspond to the strongest edge along each search line, without guaranteeing that they belong to the object boundary. Consequently, the total number of detected observation points is typically greater in the EM-RASM approach.

4.1 Performance Measures

The segmentations were evaluated by comparing the obtained contours with the true object boundary (ground truth). The accuracy of the segmentations were

quantitatively determined by using the Dice coefficient [15], and the average distance of each model point to the ground truth. The former metric measures the agreement between two contours as follows. Let R_1 be the region delimited by the first contour and R_2 the region delimited by the second contour. The Dice coefficient is computed as follows

$$D(R_1, R_2) = 2\frac{A(R_1 \cap R_2)}{A(R_1) + A(R_2)}, \tag{16}$$

where $A(\cdot)$ denotes the area of the region and $\cap$ denotes the intersection. A Dice coefficient of 1 means there is a perfect match between the two contours and a value of 0 means the corresponding regions do not even overlap.

4.2 Left Ventricle Segmentation

We applied the EM-RASM method in the segmentation of the left ventricle in 2D ultrasound image sequences. The dataset is composed of five 2D sequences (five different patients), each with 16-20 frames. The shape model was trained using medical annotations of the left ventricle contours (ground truth). Each training example was obtained by resampling, in arc-length, the medical contours with a fixed number of points from the bottom left to the apex (top) and from the bottom right to the apex. We tested the proposed algorithm and the standard ASM using a leave-one-sequence-out scheme, i.e., learning the shape model with four sequences and testing in a fifth, and repeating this for each test sequence.

As previously mentioned, the initial guess for the transformation parameters was obtained by aligning the average contour $\bar{\mathbf{x}}$ with a contour obtained by human input using the standard least squares method. A different human input contour was used for each test sequence, and the resulting initial guess was used in all the frames of the sequence (i.e., we did not propagate the contours from one frame to the next).

Table 1. Performance statistics for the segmentation of the LV: average value and standard deviation

	ASM	EM-RASM
Dice coefficient	0.78 (0.06)	**0.88** (0.04)
Average distance	20.4 (4.6)	**10.3** (3.0)

Figure 1 (top) shows four examples of the segmentation obtained with EM-RASM and with the standard ASM. In all the examples, a large number of the detected observations (red dots) were outliers. The figure shows that the EM-RASM performed better than the standard ASM and was able to fit the

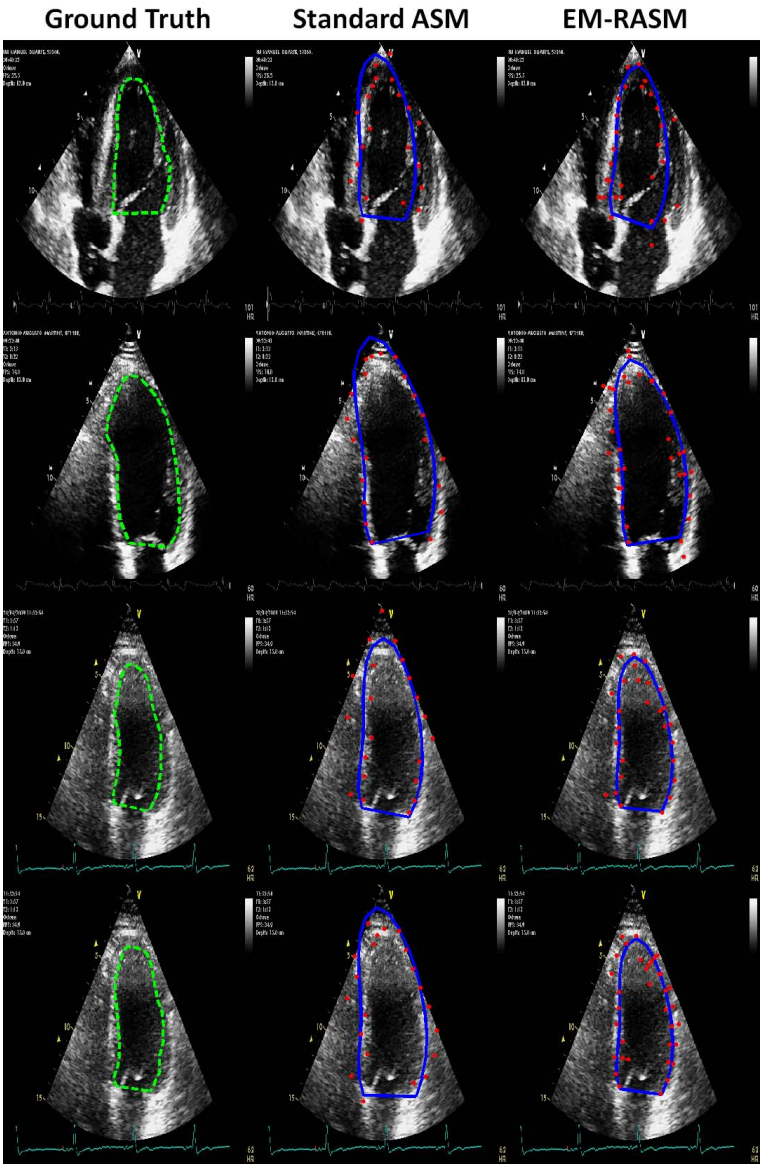

Fig. 1. Segmentation of the left ventricle in ultrasound images. The green dashed line shows the ground truth and the blue lines correspond to the estimated contour. The red dots represent the detected observations in the last iteration.

LV boundary, whereas the contour obtained using the standard ASM was hampered by the outliers. Statistical results are presented in Table 1 and in the boxplots of Figure 2, showing that the EM-RASM method, leads to a significant improvement in the segmentation accuracy.

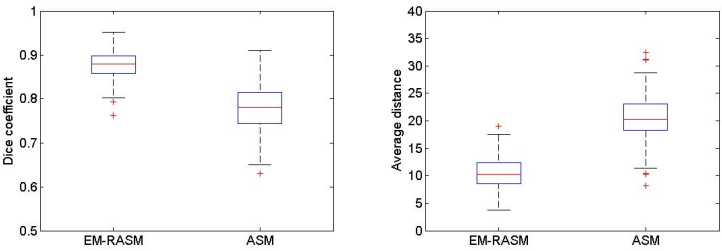

Fig. 2. Boxplots of the error metrics for the segmentation of the left ventricle in ultrasound images (the average distance is measured in pixels)

5 Conclusion

This paper combines active shape models (ASM) with robust estimation of the model pose and deformation using an outlier model. The estimation of the model parameters is achieved using the EM method, that assigns confidence degrees (weights) to each observation and take confidence degrees into account during the estimation of the model parameters. We show that this approach is robust in the presence of outliers since outlier observations tend to receive confidence degrees close to zero and have a small influence on the model estimates.

Future work should focus on extending the proposed framework to more reliable observations, such as edge strokes [12]. Since edge points along the same edge often belong to the same object in the image, the computation of the weights associated to observations can be improved. The use of application-specific features is another direction to be explored.

References

1. Cootes, T.F., Taylor, C.J., Cooper, D.H., Graham, J.: Active shape models-their training and application. Computer Vision and Image Understanding 61(1), 38–59 (1995)
2. Cootes, T.F., Edwards, G.J., Taylor, C.J.: Active appearance models. IEEE Transactions on Pattern Analysis and Machine Intelligence 23(6), 681–685 (2001)
3. Van Ginneken, B., Frangi, A.F., Staal, J.J., ter Haar Romeny, B.M., Viergever, M.A.: Active shape model segmentation with optimal features. IEEE Transactions on Medical Imaging 21(8), 924–933 (2002)
4. Wimmer, M., Stulp, K., Pietzsch, S., Radig, B.: Learning local objective functions for robust face model fitting. IEEE Transactions on Pattern Analysis and Machine Intelligence 30(8), 1357–1370 (2008)
5. Cristinacce, D., Cootes, T.F.: Automatic feature localisation with constrained local models. Pattern Recognition 41(10), 3054–3067 (2008)
6. Arbeláez, P., Maire, M., Fowlkes, C., Malik, J.: Contour detection and hierarchical image segmentation. IEEE Transactions on Pattern Analysis and Machine Intelligence 33(5), 898–916 (2011)

7. Cootes, T.F., Ionita, M.C., Lindner, C., Sauer, P.: Robust and accurate shape model fitting using random forest regression voting. In: Fitzgibbon, A., Lazebnik, S., Perona, P., Sato, Y., Schmid, C. (eds.) ECCV 2012, Part VII. LNCS, vol. 7578, pp. 278–291. Springer, Heidelberg (2012)
8. Rogers, M., Graham, J.: Robust active shape model search. In: Heyden, A., Sparr, G., Nielsen, M., Johansen, P. (eds.) ECCV 2002, Part IV. LNCS, vol. 2353, pp. 517–530. Springer, Heidelberg (2002)
9. Fischler, M.A., Bolles, R.C.: Random sample consensus: A paradigm for model fitting with applications to image analysis and automated cartography. Communications of the ACM 24(6), 381–395 (1981)
10. Abi-Nahed, J., Jolly, M.-P., Yang, G.Z.: Robust active shape models: A robust, generic and simple automatic segmentation tool. In: Larsen, R., Nielsen, M., Sporring, J. (eds.) MICCAI 2006. LNCS, vol. 4191, pp. 1–8. Springer, Heidelberg (2006)
11. Chui, H., Rangarajan, A.: A new point matching algorithm for non-rigid registration. Computer Vision and Image Understanding 89(2), 114–141 (2003)
12. Nascimento, J.C., Marques, J.S.: Adaptive snakes using the EM algorithm. IEEE Transactions on Image Processing 14(11), 1678–1686 (2005)
13. Dempster, A.P., Laird, N.M., Rubin, D.B.: Maximum likelihood from incomplete data via the em algorithm. Journal of the Royal Statistical Society. Series B (Methodological), 1–38 (1977)
14. Blake, A., Isard, M.: Active shape models. Springer (1998)
15. Dice, L.R.: Measures of the amount of ecologic association between species. Ecology 26(3), 297–302 (1945)